Atmosphere–Land Surface Interactions over the Southern Great Plains: Characterization from Pentad Analysis of DOE ARM Field Observations and NARR

ALFREDO RUIZ-BARRADAS

Department of Atmospheric and Oceanic Science, University of Maryland, College Park, College Park, Maryland

SUMANT NIGAM

Department of Atmospheric and Oceanic Science, and Earth System Science Interdisciplinary Center, University of Maryland, College Park, College Park, Maryland

(Manuscript received 12 July 2011, in final form 24 July 2012)

ABSTRACT

The Department of Energy Atmospheric Radiation Measurement Program (ARM) Southern Great Plains (SGP) site data are analyzed to provide insight into atmosphere–land surface interactions generating summertime precipitation variability. Pentad-averaged (5 days) data are analyzed; the average is long enough to suppress synoptic variability but sufficiently short to resolve atmosphere–land surface interactions. Intercomparison with the precipitation-assimilating North American Regional Reanalysis (NARR) helps with in-depth investigation of the processes. The analysis seeks to ascertain the process sequence, especially the role of evapotranspiration and soil-moisture–radiation feedbacks in the generation of regional precipitation variability at this temporal scale.

Transported moisture dominates over evapotranspiration in precipitation variability over the region, from both magnitude of the contribution to regional water balance and its apparent temporal lead at pentad resolution. Antecedent and contemporaneous evapotranspiration are found to be negatively correlated with precipitation, albeit statistically insignificant; only lagging correlations are positive, peaking at 2-pentad lag following precipitation, substantiating the authors' characterization of the water balance over SGP, and extending the authors' previous findings on the dominance of moisture flux convergence in generating precipitation variability at monthly scales.

Precipitation episodes are linked with net negative surface radiation anomalies (i.e., with an energy-deprived land surface state that cannot fuel evapotranspiration), ruling out radiatively driven positive feedback on precipitation. Although the net longwave signal is positive because of a colder land surface (less upward terrestrial radiation), it is more than offset by the cloudiness-related reduction in downward shortwave radiation. Thus, ARM (NARR) data do not support the soil-moisture–precipitation feedback hypothesis over the SGP at pentad time scales; however, it may work at subpentad resolution and over other regions.

1. Introduction

The U.S. Great Plains is a region of heightened atmosphere–land surface interaction from boreal spring to fall. Terrestrial water resources are recharged in winter/spring and expended in summer and fall (the growing seasons), with evapotranspiration being a key element of the seasonal regional atmospheric and terrestrial water cycles (e.g., Nigam and Ruiz-Barradas 2006). However, evapotranspiration has a modest role in nonseasonal hydroclimate variability over this region. Ruiz-Barradas and Nigam (2005, hereafter RBN05), for instance, show remote water sources (transported moisture and related convergence) to be more important than local ones (evapotranspiration) in observed precipitation variability.

Atmosphere–land surface models, in contrast, accord evapotranspiration a prominent role in nonseasonal hydroclimate variability. Not surprisingly, most climate models are unable to simulate with any fidelity the observed hydroclimate variability record (including multiyear droughts), even when variations are averaged over a large domain (e.g., the >1 000 000 km^2 Great Plains

Corresponding author address: Alfredo Ruiz-Barradas, 3405 Computer and Space Sciences Building, University of Maryland, College Park, College Park, MD 20742-2425.
E-mail: alfredo@atmos.umd.edu

DOI: 10.1175/JCLI-D-11-00380.1

region). The problematic portrayal of nonseasonal variability in models includes vigorous recycling of local precipitation (RBN05; Ruiz-Barradas and Nigam 2006b, hereafter RBN06b), a manifestation of intense local atmosphere–land surface coupling, which distorts the regional water balance: Leading terms in the anomalous atmospheric balance are precipitation and moisture flux convergence in observations and precipitation and evapotranspiration in model simulations. Heightened atmosphere–land surface interactions in models led to the notion of ''hot spots'' (Koster et al. 2004, 2006; Wang et al. 2007); the one over the Great Plains has, however, shrunk/retreated westward with model improvements (Dirmeyer et al. 2009; Dominguez et al. 2006; Zeng et al. 2010). (''Hot spots'' is an interesting name, since precipitation recycling in the models often leads to colder land surface states, given the intertwined water and energy cycles.)

The present study seeks to reveal the process sequence governing atmosphere–land surface interaction from analysis of the spatiotemporal relationships of pentad-averaged hydroclimate variables. The use of pentad averages allows focus on supersynoptic variability, an influential variability component between synoptic and monthly time scales (e.g., Weaver and Nigam 2011). Analysis of pentad-averaged hydroclimate fields can reveal the significance of atmosphere–land surface interaction on time scales longer than the diurnal ones where this interaction is relevant (e.g., Findell et al. 2011). Interestingly, the significance of this interaction is not as clear on longer time scales (e.g., RBN05), including the daily one (e.g., Salvucci et al. 2002; Wei et al. 2008). The 5-day (or pentad) averaging is long enough to suppress the fast convection and cloud time scales and, to an extent, synoptic variability but short enough to resolve the interactions of atmospheric and terrestrial hydroclimate variables (precipitation, surface shortwave and longwave radiation, evaporation, column moisture flux, and surface air temperature).

Another unique feature of this study is the use of field data [from the Atmospheric Radiation Measurement Program (ARM) Southern Great Plains (SGP) site] to investigate atmosphere–land surface interaction. The interaction is typically studied using models and atmospheric reanalyses, that is, model-influenced datasets. Reanalysis data are characterized in this manner because hydroclimate variables are seldom assimilated (i.e., observationally constrained) in atmospheric reanalysis and, as such, heavily influenced by the assimilating model's physical parameterizations (e.g., precipitation). One reanalysis dataset we do analyze along with the ARM SGP field observations is the National Oceanic and Atmospheric Administration (NOAA) North American Regional Reanalysis (NARR; Mesinger et al. 2006). NARR is different from canonical reanalyses because it assimilates precipitation and radiances successfully (Ruiz-Barradas and Nigam 2006a, hereafter RBN06a), nudging hydroclimate variables closer to observations. Precipitation assimilation in NARR is accomplished by nudging precipitation, humidity, temperature, and cloud water mixing ratio but not soil moisture. Land surface's influence on precipitation, through evaporation, is thus ignored during the assimilation process, and this is not without consequence for the atmospheric water balance, as discussed in Nigam and Ruiz-Barradas (2006). In addition, albedo varies with snow cover and clouds but not soil moisture. For all these reasons, the NARR climatological evaporation is larger than offline estimates (Nigam and Ruiz-Barradas 2006). Although NARR may not be the ideal dataset to investigate precipitation–soil-moisture feedbacks (Luo et al. 2007), it is the best precipitation-assimilated reanalysis that we currently have and, as such, is used here to provide large-scale context. Intercomparison with field observations helps with NARR validation but, more importantly, allows spatial ''continuance'' of the results obtained from analysis of the subgrid-scale SGP field data on to more expansive regional domains (e.g., SGP).

The targets of this observationally rooted, pentad-resolution lead–lag analysis of atmosphere–land surface interactions are (i) characterization of the nature of the atmospheric water balance and (ii) assessment of the viability of the soil-moisture–precipitation feedback hypothesis (e.g., Eltahir 1998) that is driven by receipt of excessive net radiative energy at the wet and colder land surface. Advancing understanding of the process sequence underlying such interactions should facilitate improvements in models' physical parameterizations, especially of thermodynamic processes operating in the atmospheric column. As column thermodynamics both influences and is influenced by the land surface state, the fast convection and cloud processes cannot be easily separated from the slower atmosphere–land surface interactions unfolding at the column base.

The paper is organized as follows. Section 2 describes the datasets while section 3 shows the study region and the hydroclimate components of atmospheric water balance associated with nonseasonal pentad precipitation variability in summer. The NARR and ARM surface radiation and hydroclimate fields are shown in section 4, which also assesses the viability of the soil-moisture–precipitation feedback hypothesis. Lead–lag links of precipitation with the water-cycle and surface radiation fields are shown in section 5. Concluding remarks follow in section 6.

2. Datasets and analysis method

The analysis of atmosphere–land surface interactions is carried out using several datasets. Important features of the datasets, including their processing, are described next.

a. NARR dataset

The NARR is a long-term, consistent, data-assimilation-based climate data suite for North America (Mesinger et al. 2006). It is produced at high spatiotemporal resolution (32 km, 45 layers, and 3-hourly) and spans a period of more than 30 yr, from October 1978 to the present; it is based on the April 2003 frozen version of the National Centers for Environmental Prediction (NCEP) mesoscale Eta forecast model and the Eta Data Assimilation System (EDAS). The NARR assimilates radiances and precipitation. Assimilation of precipitation is, in fact, successful, with downstream effects, including two-way interaction between precipitation and the improved land surface model (Ek et al. 2003; Mitchell et al. 2004). Even so, NARR produces somewhat larger evapotranspiration (Nigam and Ruiz-Barradas 2006). The NARR dataset has been extrapolated to a $0.5° \times 0.5°$ grid for this analysis. Moisture fluxes and related convergence were calculated at 21 vertical levels from the surface to 300 hPa and then vertically integrated. Fractional volumetric soil moisture was extracted at each of the four layers; however, only the surface–0.1-m-layer soil moisture is used in the present analysis.

b. ARM Southern Great Plains data

Data from the ''extended facilities'' in the Southern Great Plains, and belonging to the energy balance Bowen ratio (EBBR; Cook 2007) observing system are used. The EBBR system is designed to produce 30-min estimates of the vertical fluxes of sensible and latent heat at the local surface but also provides measurements of soil temperature, moisture, and heat fluxes in the upper 0.05 m of the soil; net radiation and surface air temperature are also measured. Consistent data for the period 1996–2002 were analyzed after homogenizing the station data on to a $0.5° \times 0.5°$ grid. In addition to analysis of atmosphere–land surface interaction, data from ARM (Stokes and Schwartz 1994) are used for validation of the NARR soil-moisture and radiative fluxes.

c. Climate Prediction Center precipitation analysis

The gridded ($1° \times 1°$) precipitation observations used in this analysis come from the NCEP Climate Prediction Center (CPC) retrospective analysis of daily station precipitation over the United States and Mexico (referred to as the U.S.–Mexico dataset; Higgins et al. 1996, 2000) for the 1948–present period.

d. Pentad averaging

Pentads are created by averaging data in 5-day groups for each year, starting on 1 January. The last pentad in February starts on 25 February of each year and finishes on 1 March; in a leap year, however, a hexad is formed by including 29 February. A 7-yr (1996–2002) climatology is constructed at pentad resolution, from which pentad anomalies are computed for each year. The summer season is taken to begin at pentad 32 (5–9 June) and end on pentad 49 (29 August–2 September). Seven summers (1996–2002) of pentad data are analyzed; due to the short analyzed period, the present analysis could be considered a case study, but the analysis of the NARR data for the longer period 1979–2002 (not shown) gives very similar results to those shown in the following sections.

e. Regressions

Regional summer precipitation variability for the central United States was tracked by creating indices over three different domains as area averages of summer pentad precipitation anomalies (Fig. 1). Because of relatively high correlation among the indices, only one was chosen to be displayed showing regressions. Regressions on water- and radiation-related fields were then calculated by using this precipitation index to identify the spatial structure of these fields associated with the variability of the index.

3. Southern Great Plains hydroclimate variability

The range of hydroclimate variability is typically, and easily, assessed using the standard deviation (STD) measure. The precipitation STD for the summer pentads from the U.S.–Mexico station data is shown in Fig. 1. The variability is large where the climatology is large: for example, over the central United States (not to mention eastern Mexico), where pentad STD is as large as the climatology. The monthly STD here is only 50% of the climatology and focused in the northern Great Plains (GP) box (35°–45°N, 100°–90°W; see RBN05) shown in gray in Fig. 1a. The ARM Southern Great Plains (ASGP) site is located in the southwestern corner of the GP box (34.5°–38.5°N, 99.5°–95.5°W) and is outlined in black in Fig. 1a. It encompasses the core of the pentad precipitation variability region. Also shown in Fig. 1a is another box, in white, that extends almost equally on all sides of the ASGP site; this is called the southern Great Plains

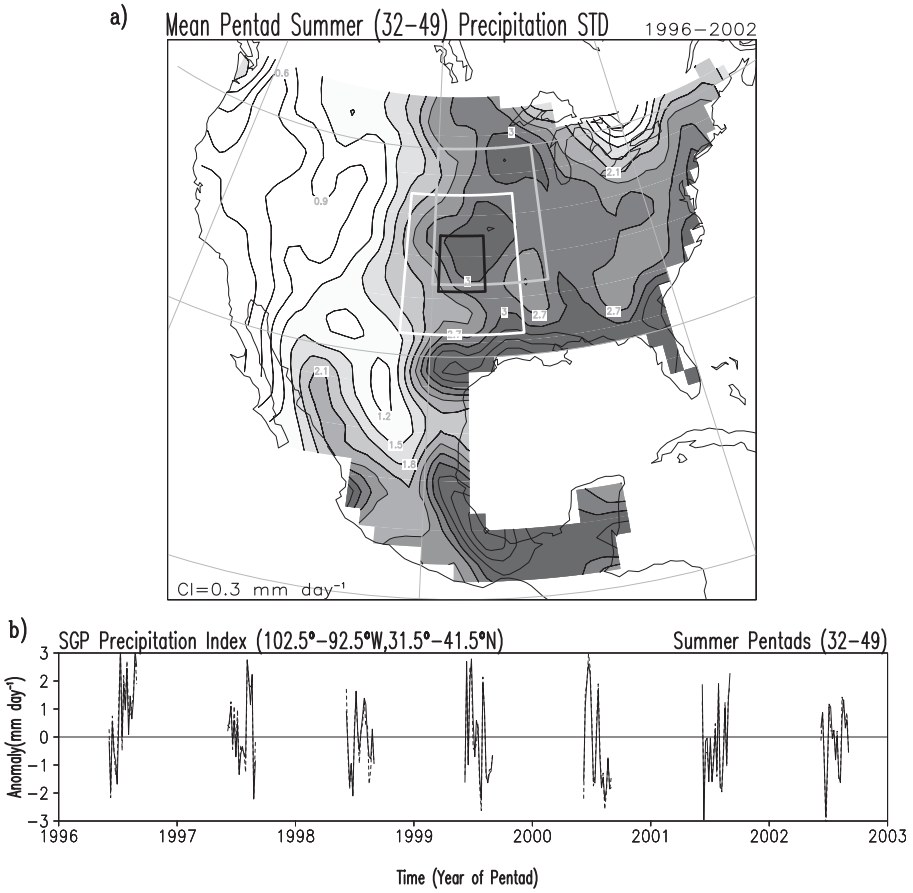

FIG. 1. (a) Mean standard deviation of summer pentad precipitation for the 1996–2002 period from the CPC U.S.–Mexico retrospective precipitation analysis. The mean is obtained from the 18 standard deviations of precipitation pentads 32–49 (5–9 Jun to 29 Aug–2 Sep). Contour interval is 0.3 mm day^{-1} and shading is for contours equal to or larger than 1.2 mm day^{-1}. For displaying purposes, the field has been smoothed via the Grid Analysis and Display System (GrADS) nine-point smoother smth9. Boxes over the central United States denote 1) GP region in gray (as used in RBN05 and enclosing the region of maximum summer standard deviation, 35°–45°N, 100°–90°W); 2) the ASGP domain in black (34.5°–38.5°N, 99.5°–95.5°W); and 3) the SGP region in white, enclosing entirely the ASGP domain and a large portion of the GP domain (31.5°–41.5°N, 102.5°–92.5°W). (b) Area-averaged summer pentad precipitation anomalies over the SGP domain defining the SGP pentad precipitation index; the continuous line is from the CPC dataset while the dashed line is from the NARR dataset.

(SGP) box (31.5°–41.5°N, 102.5°–92.5°W). Both big boxes cover more than 10^6 km^2 each. The SGP and the inner ASGP boxed regions will be the focus of the ensuing analyses.

As the STD distribution does not provide insights into the spatiotemporal structure of variability, the SGP domain is used to create an area-averaged precipitation anomaly index that can characterize regional temporal variability and the structure of related hydroclimate and radiative fields through regressions. The SGP precipitation index from U.S.–Mexico station data and NARR is displayed in Fig. 1b at pentad resolution; the indices are highly correlated (0.97), reflecting successful assimilation of precipitation in NARR. The observed precipitation indices from the three marked boxes are also well correlated: r(GP, SGP) = 0.7, r(GP, ASGP) = 0.6, and r(SGP, ASGP) = 0.8.

The presence of a coherent observed precipitation anomaly in the SGP box (Fig. 2a) is not surprising, given the index definition. The nature of anomalous atmospheric water balance can be surmised from the related moisture flux convergence and evapotranspiration regressions (Figs. 2b,c; note the smaller contour interval in Fig. 2c), both from NARR. Moisture flux convergence dominates evapotranspiration, almost completely, over the ASGP box and over the central–eastern SGP box on pentad time scales, much as on monthly time scales

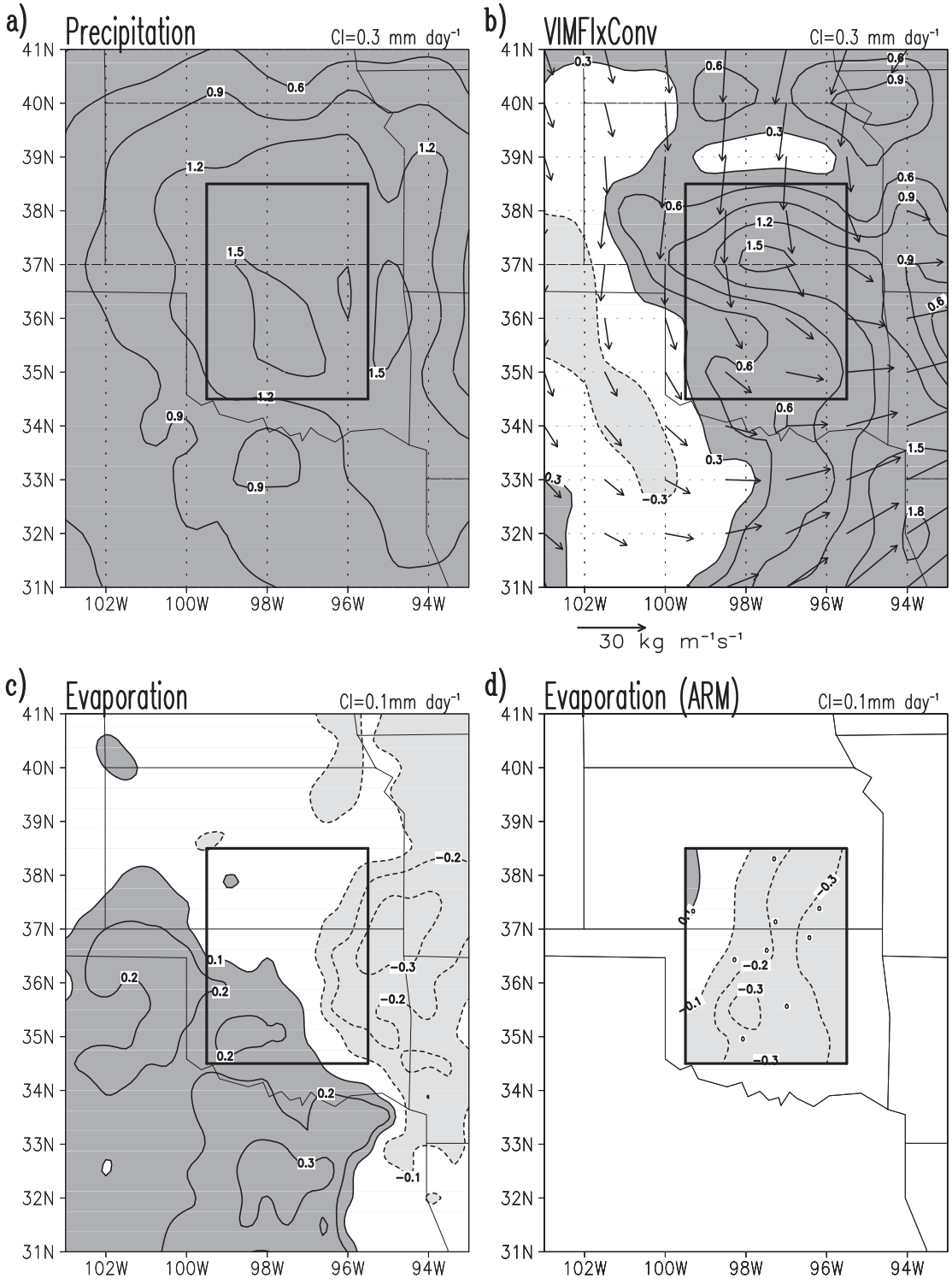

FIG. 2. Regressed NARR and ARM anomalies on the SGP observed summer pentad precipitation index for the 1996–2002 period over the SGP region: (a) precipitation, (b) vertically integrated moisture flux and total moisture flux convergence, (c) evaporation from NARR dataset, and (d) evaporation from the ARM EBBR dataset. The outlined box encloses the ARM SGP domain, and the dots in the ARM panel indicate the stations used in the dataset. Contour interval is 0.3 mm day^{-1} and values equal to or larger than $|\pm 0.3|$ mm day^{-1} are shaded for precipitation and moisture flux convergence. Similarly for evaporation, a value of 0.1 mm day^{-1} is used. Positive (negative) anomalies are shaded dark (light). Moisture flux convergence has been regridded to a $1° \times 1°$ grid for displaying purposes. The moisture flux scale is shown at the bottom of (b).

(RBN05; RBN06a). NARR evapotranspiration exhibits a coherent southwest–northeast dipole structure but is weak (~0.3 mm day^{-1}) vis-à-vis column moisture flux convergence and precipitation anomalies. The corresponding ARM SGP site evapotranspiration anomalies (Fig. 2d) are westward shifted but otherwise similar to NARR's: for example, the similar west–east gradient and magnitudes. The ARM field data show evapotranspiration anomalies over the ASGP box to be, in fact, negative.

The ARM SGP field measurements of evapotranspiration provide valuable reading on an elusive quantity, one variedly represented in model simulations and reanalyses (Nigam and Ruiz-Barradas 2006; RBN05). The readings, especially magnitude, contribute to a definitive characterization of the nature of nonseasonal atmospheric water balance, which is dominated by the relationship between precipitation and column moisture flux convergence. A profound role for moisture transports is thus indicated.

4. Precipitation, soil wetness, and surface radiation and air temperature

Nonseasonal precipitation episodes lead, as they must, to a wet land surface state. Regressions of the pentad SGP precipitation index on NARR and ARM volumetric water content (VWC) are displayed in Figs. 3a,b; both indicate similar wetness (~2%), but with more texture in ARM regressions.[1] The wetter soil is, interestingly, accompanied by less net surface radiation in both NARR and ARM datasets (Figs. 3c,d): that is, an energy-deprived land surface state. The net radiation anomalies have a west–east gradient, much as in the evapotranspiration regressions (cf. Fig. 2d). This is indicative of the radiative control on evapotranspiration, an assertion supported by the magnitude of the involved anomalies as well: 8–10 W m^{-2} of net radiative deficit in the eastern sector of the ASGP box is linked with a 0.3 mm day^{-1} evapotranspiration deficit, entirely consistent with energy requirements (1 mm day^{-1} of evaporation needs 28.94 W m^{-2}).[2] The plots also indicate that a net radiative surplus is not essential for evapotranspiration; for example, positive anomalies in the southwest sector of the SGP box occur in a region of weak but slightly negative net surface radiation anomalies. Sensible heat flux into the ground, anchored by cold surface temperatures (Figs. 3e,f), may well be important in such regions.

The surface radiation budget is examined more closely in Fig. 4, which shows the related shortwave and longwave components, all from NARR for reasons of availability. The biggest component is downward shortwave (Fig. 4d), which is focused somewhat southeastward of the ASGP precipitation; its large negative values represent reduction from precipitation-related increased cloudiness. The net shortwave (Fig. 4b) is smaller but similarly structured, suggesting the albedo offset. As mentioned in the introduction, the albedo itself does not change because of soil moisture in NARR, but a similar analysis with NCEP/Department of Energy (DOE) Global Reanalysis 2 (Kanamitsu et al. 2002) indicates a small albedo[3] increase of 2% in the SGP core region (not shown), questioning the wet-soil–decreased-albedo–increased-precipitation hypothesis of Eltahir (1998), who did not factor for the cloudiness-related reduction in downward shortwave radiation (cf. Fig. 4d); the author's subsequent modeling study (Zheng and Eltahir1998) did, however, recognize the role of clouds. Regardless, our observational analysis (ARM and NARR) does not support a critical element of Eltahir's soil-moisture–precipitation feedback hypothesis, as the precipitation-related net surface shortwave radiation anomaly (Fig. 4b) is strongly negative over the precipitating region (from cloud cover and, apparently, no albedo-related offset). [The corresponding net surface longwave and shortwave anomalies from the NCEP/DOE Global Reanalysis 2 are also positive and negative, respectively, but associated with purely positive evaporation anomalies (not shown).]

The net surface longwave anomaly, on the other hand, is focused a bit to the southwest of ASGP precipitation. To a large extent, it is shaped by reduced upward emissions from the colder land surface (Fig. 4c), along with some increased downward emission from increased atmospheric humidity and cloudiness (not shown), much as Eltahir (1998) proposed. Although this element of his feedback hypothesis is corroborated, net surface radiation from both longwave and shortwave components is negative (cf. Fig. 3c), generating an energy-deprived

[1] Although NARR and ARM have similar VWC, note that the NARR values are for the surface–0.1-m layer and, as such, represent greater water holding than those from the ARM dataset that are measurements at a 0.05-m depth. This can lead to excessive evapotranspiration (e.g., Nigam and Ruiz-Barradas 2006) and less runoff (see unpublished work online at http://www.atmos.umd.edu/~alfredo/sfcwatbal_unpublished.pdf).

[2] 1 mm day^{-1} = 1 kg m^{-2} day^{-1} of water. Energy for evaporation of 1 mm day^{-1} = $1 \times L_v$ J m^{-2} day^{-1}, where L_v is the latent heat of condensation (=2.5×10^6 J kg^{-1}). Energy needed for evaporation is thus (2.5×10^6)/86 400 J s^{-1} m^{-2} or 28.94 W m^{-2}.

[3] Albedo calculated as the ratio of surface upward shortwave radiation to surface downward shortwave radiation from NCEP/DOE Global Reanalysis 2.

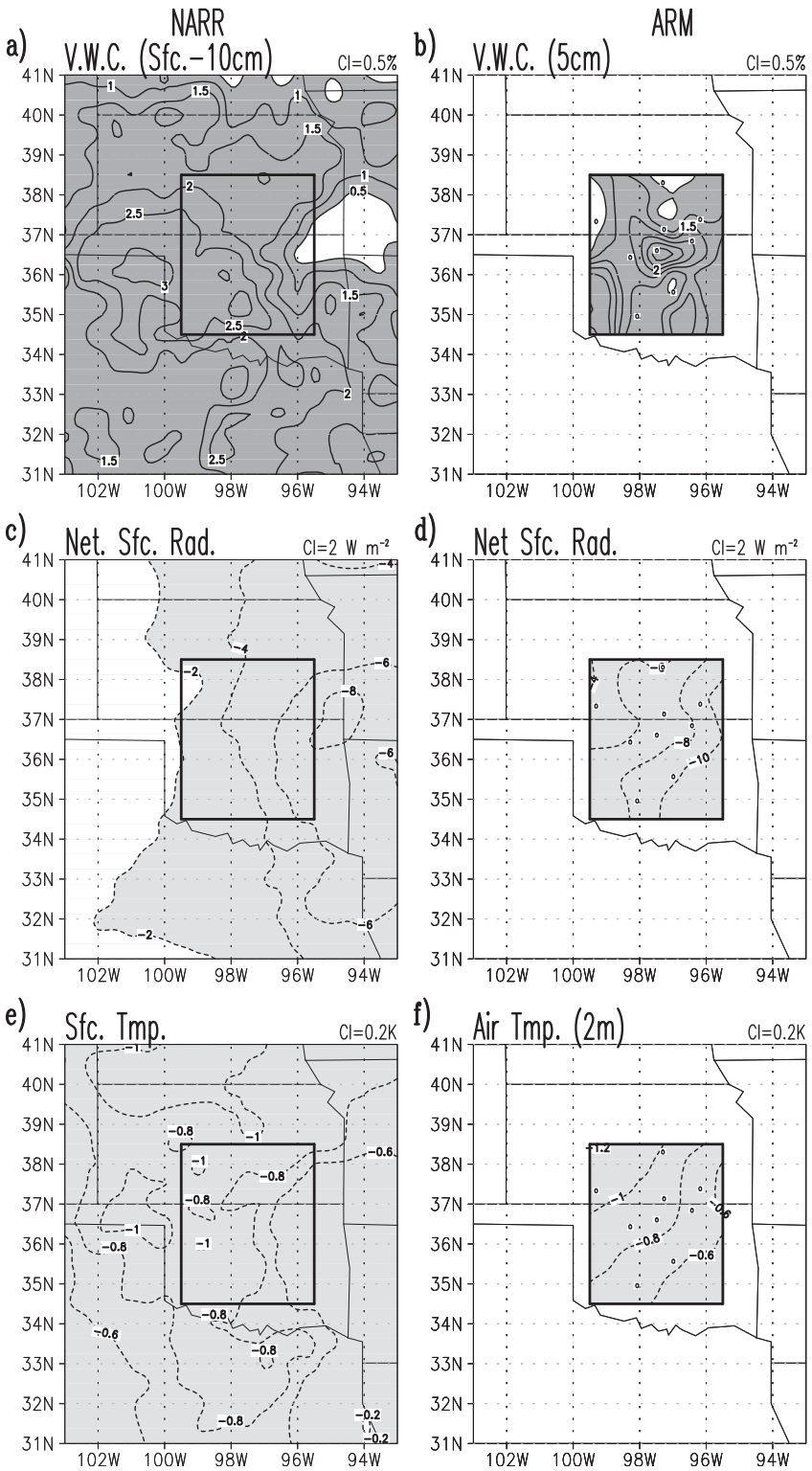

FIG. 3. Regressed NARR and ARM anomalies on the SGP summer pentad precipitation index for the 1996–2002 period over the SGP region: (a) volumetric water content in the surface–0.1-m layer, (c) net surface radiation, and (e) surface temperature from the NARR dataset and (b) volumetric water content at 0.05-m depth, (d) net surface radiation, and (f) air temperature at 2 m from the ARM EBBR dataset. The outlined box encloses the ARM SGP domain, and the dots in the ARM panels indicate the stations used in the dataset. Contour interval is 0.5% and values equal to or larger than $|\pm 0.5|$ % are shaded for the volumetric water content with positive anomalies in dark shading. Similarly, for net surface radiation and temperature, contour intervals of 2 W m^{-2} and 0.2 K, respectively, are used with negative anomalies in light shading.

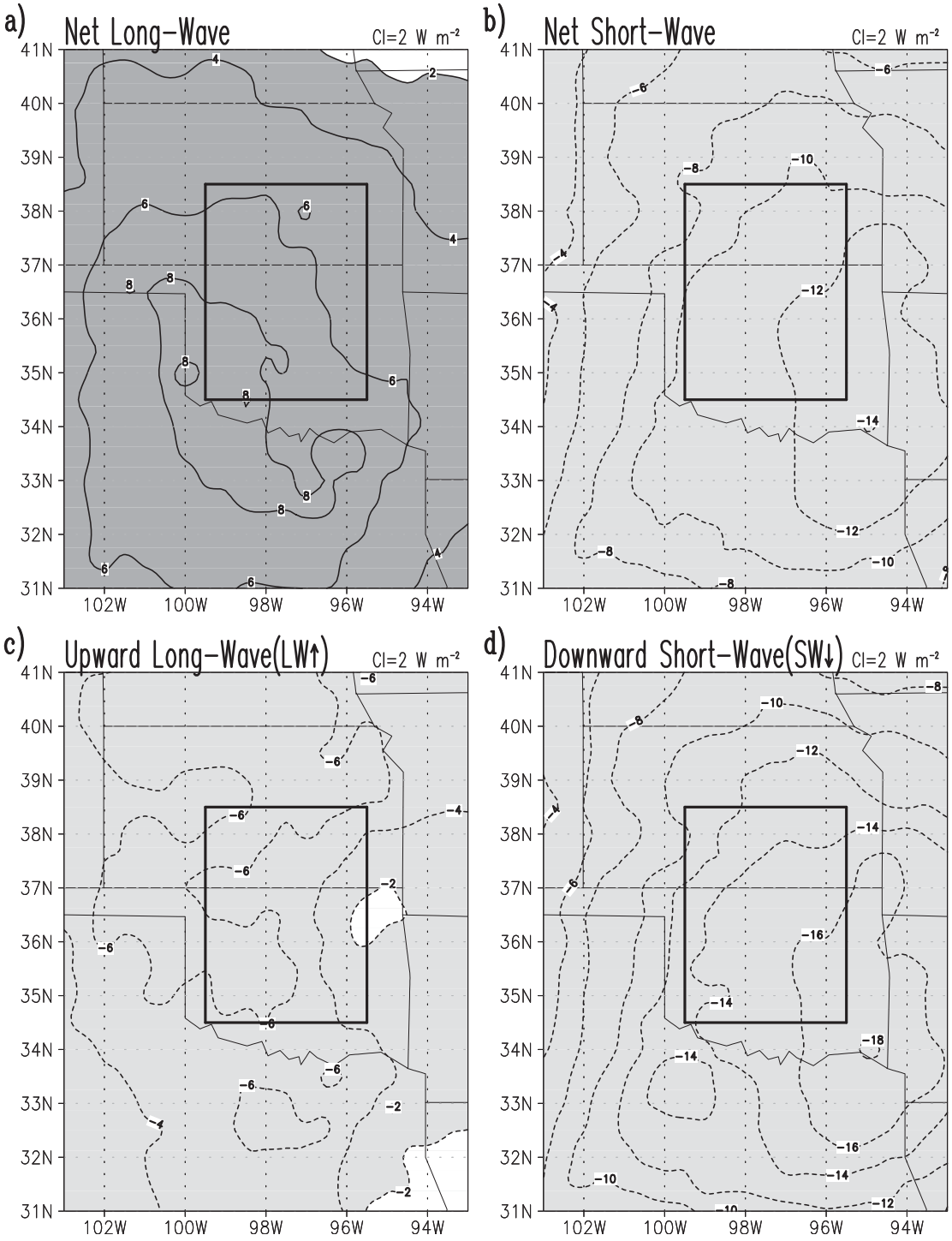

FIG. 4. Regressed NARR surface radiative anomalies on the SGP summer pentad precipitation index for the 1996–2002 period over the SGP region: (a) net longwave and (b) net shortwave surface radiation, (c) upward longwave surface radiation, and (d) downward shortwave surface radiation. The outlined box encloses the ARM SGP domain. Contour interval is 2 W m^{-2} and values equal to and larger than $|\pm 2|$ W m^{-2} are shaded dark (light) for positive (negative) anomalies.

environment over the central–eastern portion of the SGP box. In the western sector, the increase in net longwave radiation offsets the net shortwave signal, almost completely, creating an energy-neutral environment that permits weak evapotranspiration (cf. Fig. 2c; note the smaller contour interval). As indicated from Figs. 2a,b, the moisture for precipitation comes largely from moisture transports.

5. Pentad lead–lag relationship between precipitation and surface hydroclimate

More insight into the process sequence operating prior to and concurrently with anomalous SGP precipitation events is obtained from their pentad-resolution lead–lag links; anomalies for both precipitation and linked variables (from NARR and ARM) are averaged over the ASGP box. Links with the water cycle are shown in Fig. 5a. The antecedent NARR and ARM evapotranspiration is negatively correlated with precipitation: for example, ~ -0.2 at 1-pentad lead, which is even larger (~ -0.4) at zero lag for the ARM field; the NARR field is, however, uncorrelated at zero lag. Column moisture flux convergence (from NARR), on the other hand, leads precipitation (1-pentad lead correlation ~ 0.3); the positive correlation is even larger at zero lag (~ 0.4).

The soil moisture exhibits peak correlation with precipitation after some delay, as expected from preceding dryness; ARM and NARR volumetric water contents are maximally correlated (~ 0.6) at 1-pentad lag in Fig. 5a. Intuitively, evapotranspiration must lag soil moisture, and it does, attaining peak correlations (~ 0.4) with precipitation at 2-pentad lag. Its lag vis-à-vis soil moisture reflects only that it is at the latter's expense.

Pentad analysis shows clear dominance of transported moisture over evapotranspiration in nonseasonal precipitation variability at the SGP field site (and more broadly over SGP), from both magnitude of the contribution to regional water balance and its apparent temporal lead at pentad resolution. Such temporal leads have been noted in context of the 1988 drought and 1993 flood over the Great Plains (Weaver et al. 2009) as well as during hydroclimate episodes linked with supersynoptic fluctuations of the Great Plains low-level jet (Weaver and Nigam 2011). Antecedent and contemporaneous evapotranspiration are, in fact, found to be negatively correlated with precipitation; only lagging correlations are positive, peaking at 2-pentad lag (i.e., following precipitation), lending support to our characterization of the water balance over SGP at pentad resolution. Although statistical significance cannot be fully established from the short record of observations, it is important to note the sign of the correlation, in particular that it is maximum positive not at zero lag but later. Although this will need to be confirmed with longer datasets, it is already suggestive of the hydrodynamic process sequence in play over the southern Great Plains. Thus, the characterization is no different from that posited in RBN05 for the central Great Plains based on extensive analysis of monthly averaged observations/reanalysis data.

The modest correlation of precipitation with evapotranspiration and moisture flux convergence (i.e., with squared correlations not adding up to 1.0) raise the question of how pentad variability of precipitation is generated in NARR. The accounting question would be pertinent if NARR exhibited a balanced atmospheric water budget. Nigam and Ruiz-Barradas (2006), however, show that the budget over this region is unbalanced in the monthly climatology; there is no reason to expect balance on the submonthly time scales. Our analysis suggests that the imbalance could well result from subtle misrepresentation of the temporal lead/lag among key hydroclimate variables (e.g., among P and E in NARR vs ARM; see Fig. 5a).

Lead–lag links of precipitation with the surface radiation fields are shown in Fig. 5b. Unlike water-cycle fields in Fig. 5a, the radiation ones exhibit significant (and peak) correlations only at zero lag, indicating the comparatively faster convection, cloud, and radiation time scales. The simultaneous precipitation–surface radiation relationships have all been noted earlier in discussions of Figs. 3 and 4. Note, the net surface radiation does become positively correlated (~ 0.2) with precipitation at 2-pentad lag but largely from the abatement of cloudiness; the net longwave is correlated at close to zero at this time. Dominance of the cloud-mediated surface shortwave signal at both zero and 2-pentad lag leaves little support for the soil-moisture–precipitation feedback hypothesis. A finer temporal sampling will be needed to assess its viability on shorter time scales.

The lead–lag correlation analysis (Fig. 5) was repeated using the NCEP/DOE Global Reanalysis 2 fields (Kanamitsu et al. 2002), where albedo is not as constrained as in NARR but precipitation is considerably less realistic. Precipitation variations, however, showed similar relationship with the radiation fields but not with the water ones (not shown). For instance, the largest correlations between the NCEP/DOE Global Reanalysis 2 precipitation and both surface-layer water content and evaporation occur contemporaneously, and not at 1–2 pentad lag as in NARR and ARM; replacing the NCEP/DOE Global Reanalysis 2 precipitation with U.S.–Mexico station precipitation does not change the relationships. In any case, the surface-layer water content anomalies are not found to lead precipitation anomalies locally.

6. Concluding remarks

The characterization of atmosphere–land surface interactions has been typically pursued in the modeling realm, stymied by the lack of regionally representative land surface observations (e.g., of evapotranspiration, soil moisture, and surface radiation) over even the Great Plains. The physical parameterizations of related

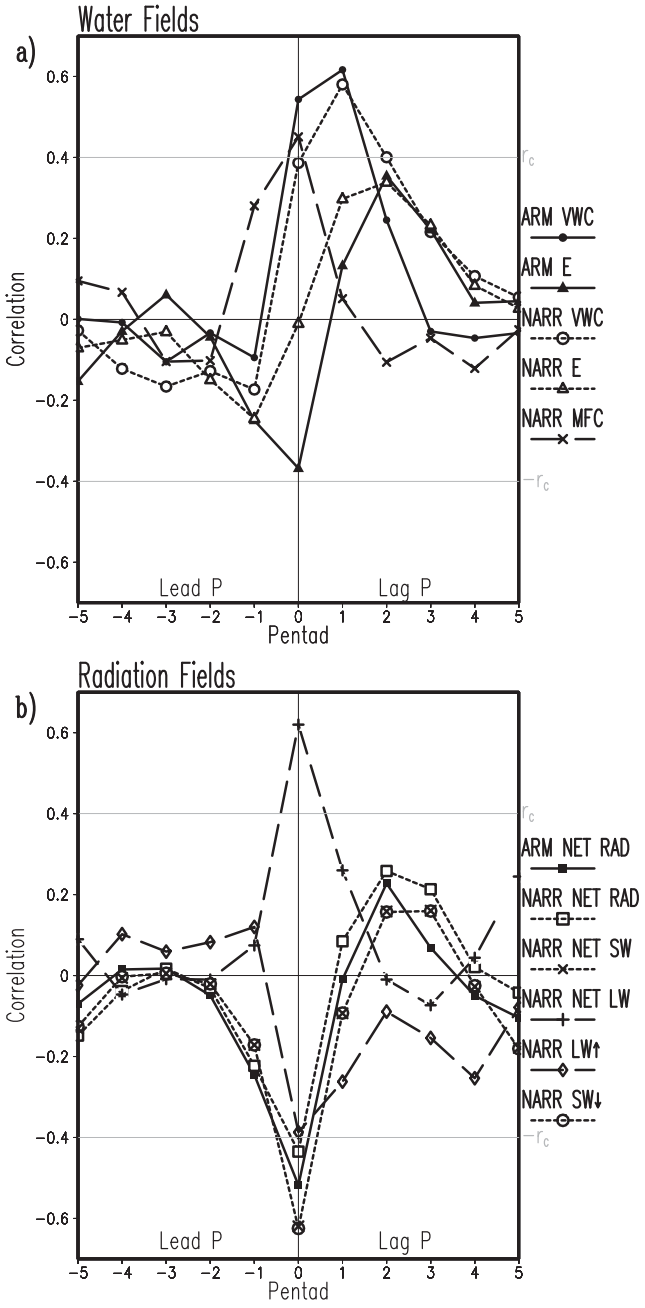

FIG. 5. Mean correlations between area-averaged pentad precipitation anomalies with anomalies of (a) water pentad fields and (b) surface radiation fields over the ARM SGP domain (34.5°–38.5°N, 99.5°–95.5°W) in summer during the period 1996–2002. Precipitation is from the CPC U.S.–Mexico retrospective dataset. (top) Correlations with the water fields include fractional volumetric water content from ARM (surface–5-cm layer: continuous line with filled circles) and NARR (surface–10-cm layer: short-dashed line with empty circles), evaporation from ARM (continuous line with filled triangles) and NARR (short-dashed line with empty triangles), and vertically integrated moisture flux convergence from NARR (long-dashed line with multiplication signs). (bottom) Correlations with surface radiation fields include net surface radiation from ARM (continuous line with filled squares) and from NARR (short-dashed line with empty squares) and net shortwave (short-dashed line with multiplication signs) and net longwave surface radiation (long-dashed line with plus signs) as well as upward longwave radiation (long-dashed line with empty diamonds) and downward shortwave radiation (short-dashed line with empty circles) from NARR. Note that correlations of precipitation with net shortwave and downward shortwave radiation are the same and only distinguishable through their multiplication and circle signs, respectively. Correlations are obtained for the 18 pentads covering the (32–49) summer pentads of each year and then averaged. Statistical significance is attained via the two-tailed Student's t test at the 0.05 level and represented by the horizontal gray line r_c ($=\pm 0.40$).

hydroclimate processes in climate models have only recently begun to be confronted with field hydrologic observations from the U.S. Department of Agriculture subgrid-scale watersheds, Oklahoma Mesonet, and the Illinois Water Survey. Valuable as they are, they do not allow a full characterization of atmosphere–land surface interactions, given their observational focus on water-cycle (and meteorology) variables.

A full characterization of atmosphere–land surface interactions, including underlying process sequences, needs observations of both water- and energy-cycle variables in view of their intertwined nature. The DOE Atmospheric Radiation Measurement Program (ARM) field site over the Southern Great Plains provides a unique, comprehensive suite of hydroclimate observations (including surface radiation) at high spatiotemporal resolution over several years to enable pursuit of a fuller characterization of pertinent interactions at pentad resolution.

The targets of this observationally rooted, pentad-resolution lead–lag analysis of atmosphere–land surface interactions are (i) characterization of the nature of the atmospheric water balance and (ii) assessment of the viability of the soil-moisture–precipitation feedback hypothesis (e.g., Eltahir 1998) that is driven by receipt of excessive net radiative energy at the wet and colder land surface. Both DOE ARM SGP field observations and data from the NOAA precipitation- (and radiance-) assimilating North American Regional Reanalysis are analyzed to meet the two targets. The NARR data was additionally analyzed so that, if validated, it could allow spatial "continuance" of the results obtained from analysis of the subgrid-scale SGP field data on to more expansive regional domains (e.g., SGP).

Robustness of the results does not to be dependent on the length of analyzed data. The analysis was repeated for the period 1979–2002 (24 yr) using only the NARR data and obtained very similar results to those displayed in the previous sections. We obtained practically the

same figures as those already seen in the paper and found that the lead–lag relationship between precipitation and the water and radiation fields is robust enough to hold for the larger period of 1979–2002.

Our pentad analysis shows the clear dominance of transported moisture over evapotranspiration in nonseasonal precipitation variability at the SGP field site (and more broadly over the SGP), from both magnitude of the contribution to regional water balance and its unambiguous temporal lead at pentad resolution. Antecedent and contemporaneous evapotranspiration are, in fact, found to be negatively correlated with precipitation but statistically not significant; only lagging correlations are positive, peaking at 2-pentad lag (i.e., following precipitation), substantiating our characterization of the atmospheric water balance over the SGP. This characterization is very similar to that put forward by the authors from analysis of monthly averaged observations for nonseasonal hydroclimate variability, which is dominated by moisture flux convergence over the central Great Plains in summer (RBN05; RBN06a).

More interestingly, our analysis finds precipitation episodes linked with net negative surface radiation anomalies (into the land surface), that is, with an energy-deprived land surface state that cannot fuel evapotranspiration. This rules out radiatively driven positive feedback on precipitation, at least, on pentad time scales. Although the net longwave signal (into the land surface) is positive because of a colder land surface (i.e., less upward terrestrial radiation), it is more than offset by the cloudiness-related reduction in downward shortwave radiation over large regions. Our analysis of ARM SGP data does not support the soil-moisture–precipitation feedback hypothesis that wet soil will elicit more precipitation locally at supersynoptic time scales; this, however, does not rule out the viability of this hypothesis at shorter (e.g., diurnal) time scales or even its existence over other regions of the planet.

This observationally rooted analysis suggests that the land surface is in an energy-limited state during precipitation episodes. Given the dominance of surface shortwave radiation over the longwave component at 0–2-pentad lags with respect to precipitation episodes, any hypothesis for atmosphere–land surface interaction, especially feedbacks, must factor for the cloud-mediated surface shortwave radiation variations.

Ignoring this shortwave signal can lead to radical misrepresentation of the atmosphere–land surface feedbacks. For example, if only longwave effects are considered, the land surface will be found to be in a radiative energy–surplus state and thus predisposed to excessive evapotranspiration and reduced runoff, broadly the very model deficiencies exhibited by atmosphere–land surface models, at least up until recently.

Acknowledgments. The authors wish to acknowledge support from the DOE and NOAA Grants DEFG0208 ER64548 and NA10OAR4310158, respectively. They also thank David Lorenz (University of Wisconsin—Madison) for sharing his archive of DOE ARM SGP site data. We also want to thank Yong-Kang Xue and two anonymous reviewers for their comments that helped to improve the paper.

REFERENCES

Cook, D. R., 2007: Energy Balance Bowen Ratio (EBBR) handbook. U.S. Department of Energy Tech. Rep. DOE/SC-ARM-TR-037, 26 pp.

Dirmeyer, P. A., C. A. Schlosser, and K. L. Brubaker, 2009: Precipitation, recycling, and land memory: An integrated analysis. *J. Hydrometeor.,* **10,** 278–288.

Dominguez, F., P. Kumar, X. Z. Liang, and M. F. Ting, 2006: Impact of atmospheric moisture storage on precipitation recycling. *J. Climate,* **19,** 1513–1530.

Ek, M. B., K. E. Mitchell, Y. Lin, E. Rogers, P. Grunmann, V. Koren, G. Gayno, and J. D. Tarpley, 2003: Implementation of Noah land surface model advances in NCEP operational mesoscale Eta model. *J. Geophys. Res.,* **108,** 8851, doi:10.1029/2002JD003296.

Eltahir, E. A. B., 1998: A soil moisture–rainfall feedback mechanism: 1. Theory and observations. *Water Resour. Res.,* **34,** 765–776.

Findell, K. L., P. Gentine, B. R. Lintner, and C. Kerr, 2011: Probability of afternoon precipitation in eastern United States and Mexico enhanced by high evaporation. *Nat. Geosci.,* **4,** 434–439, doi:10.1038/ngeo1174.

Higgins, R. W., J. E. Janowiak, and Y.-P. Yao, 1996: *A Gridded Hourly Precipitation Data Base for the United States (1963-1993).* National Centers for Environmental Prediction/Climate Prediction Center Atlas 1, 46 pp.

——, W. Shi, E. Yarosh, and R. Joyce, 2000: *Improved U.S. Precipitation Quality Control System and Analysis.* National Centers for Environmental Prediction/Climate Prediction Center Atlas 7, 40 pp.

Kanamitsu, M., W. Ebisuzaki, J. Wollen, S.-K. Yang, J. J. Hnilo, M. Fiorino, and G. L. Potter, 2002: NCEP–DOE AMIP-II Reanalysis (R-2). *Bull. Amer. Meteor. Soc.,* **83,** 1631–1643.

Koster, R. D., and Coauthors, 2004: Regions of strong coupling between soil moisture and precipitation. *Science,* **305,** 1138–1140.

——, and Coauthors, 2006: GLACE: The Global Land–Atmosphere Coupling Experiment. Part I: Overview. *J. Hydrometeor.,* **7,** 590–610.

Luo, Y., A. H. Berbery, K. E. Mitchell, and A. K. Betts, 2007: Relationships between land surface and near-surface atmospheric variables in the NCEP North American Regional Reanalysis. *J. Hydrometeor.,* **8,** 1184–1203.

Mesinger, F., and Coauthors, 2006: North American Regional Reanalysis. *Bull. Amer. Meteor. Soc.,* **87,** 343–360.

Mitchell, K. E., and Coauthors, 2004: The multi-institution North American Land Data Assimilation System (NLDAS): Utilizing multiple GCIP products and partners in a continental

distributed hydrological modeling system. *J. Geophys. Res.,* **109,** D07S90, doi:10.1029/2003JD003823.

Nigam, S., and A. Ruiz-Barradas, 2006: Seasonal hydroclimate variability over North America in global and regional reanalyses and AMIP simulations: A mixed assessment. *J. Climate,* **19,** 815–837.

Ruiz-Barradas, A., and S. Nigam, 2005: Warm season precipitation variability over the U.S. Great Plains in observations, NCEP and ERA-40 reanalyses, and NCAR and NASA atmospheric model simulations. *J. Climate,* **18,** 1808–1830.

——, and ——, 2006a: Great Plains hydroclimate variability: The view from North American Regional Reanalysis. *J. Climate,* **19,** 3004–3010.

——, and ——, 2006b: IPCC's 20th century climate simulations: Varied representations of North American hydroclimate variability. *J. Climate,* **19,** 4041–4058.

Salvucci, G. D., J. A. Salem, and R. Kaufmann, 2002: Investigating soil moisture precipitation feedbacks with tests of Granger causality. *Adv. Water Resour.,* **25,** 1305–1312.

Stokes, G. M., and S. E. Schwartz, 1994: The Atmospheric Radiation Measurement (ARM) Program: Programatic background and design of the cloud and radiation test bed. *Bull. Amer. Meteor. Soc.,* **75,** 1201–1221.

Wang, G., Y. Kim, and D. Wang, 2007: Quantifying the strength of soil moisture–precipitation coupling and its sensitivity to changes in surface water budget. *J. Hydrometeor.,* **8,** 551–570.

Weaver, S. J., and S. Nigam, 2011: Recurrent supersynoptic evolution of the Great Plains low-level jet. *J. Climate,* **24,** 575–582.

——, A. Ruiz-Barradas, and S. Nigam, 2009: Pentad evolution of the 1988 drought and 1993 flood over the Great Plains: An NARR perspective on the atmospheric and terrestrial water balance. *J. Climate,* **22,** 5366–5384.

Wei, J., R. E. Dickinson, and H. Chen, 2008: A negative soil moisture–precipitation relationship and its causes. *J. Hydrometeor.,* **9,** 1364–1376.

Zeng, X., M. Barlage, C. Castro, and K. Fling, 2010: Comparison of land–precipitation coupling strength using observations and models. *J. Hydrometeor.,* **11,** 979–994.

Zheng, X., and E. A. B. Eltahir, 1998: A soil moisture–rainfall feedback mechanism: 2. Numerical experiments. *Water Resour. Res.,* **34,** 777–785.